

**Darwin College Research Report**

---

**DCRR-001**



**An Experimental Measurement  
of the Transverse Correlation in  
Isotropic Homogenous Turbulence**

**Tamás Bertényi**

**28 November 2005**

**Darwin College  
Cambridge University  
United Kingdom CB3 9EU  
[www.dar.cam.ac.uk/dcrr](http://www.dar.cam.ac.uk/dcrr)**

**ISSN 1749-9194**

---

## ABSTRACT

This *Darwin College Research Report* provides a record of the progress in the efforts to experimentally measure the transverse correlation in an isotropic, homogenous turbulence field. The report documents - sometimes in a tedious manner - the actual experimental work completed as well as all the data gathered thus far. This was done with an eye towards future reference in the event that the effort would be attempted again. Extensive thought is given to signal processing and how it relates to real-world experimental measurements of statistical properties. Very little discussion or analysis is done on the actual results presented. Nonetheless, it should provide guidance for future continued investigations of the topic while identifying some worthy issues that merit further attention. The raw data is available from the author.

---

<sup>0</sup>KEYWORDS: transverse correlation, experimental, wind tunnel, turbulence grid, hot-wire.



# 1 Introduction

*Parturent montes, nascetur ridiculus mus*

-Horace

“... and the mountains laboured to give birth to a silly little mouse...”

This *Darwin College Research Report* documents the efforts undertaken to measure the transverse correlation in a homogenous turbulent flow-field. The motivation was to confirm and improve upon the original results of Stewart and Townsend[1]. See Davidson[2] for an excellent overview on turbulence and correlation functions. Although the project has not yet achieved these goals, interim results are presented in **Section §2 - Results**. The actual experimental apparatus and the method ultimately used to produce these results are described in detail in **Section §3 - Experimental Apparatus**. However, many alternative methods were tested and their validity evaluated; this information is presented in the embedded subsections and provides a rationale for why the final method was chosen. This rationale is particularly important if attempting to repeat and improve upon the current investigation. A brief conclusion is presented in **Section §4** with recommendations for future directions. Finally, a complete **Appendix** with the relevant data is included with descriptions of how the data is formatted. The actual data is available from the author.

## 2 Results

The final data is presented in Figure 1. This data represents 80 data points taken over a period of 34 hours on the weekend of September 26-28, 2003. The spacing between transverse points is 0.1 in terms of  $r/M$  for values up to 0.5 and then the spacing is 0.05 up to a separation of 1.5. From there onwards, the spacing is 0.25 or 0.35 until  $r/M = 2.85$  where it gradually increases to 0.1 again.

The transverse correlation,  $R$ , is plotted against normalised transverse separation,  $r/M$  where  $r$  is the transverse separation and  $M$  is the spacing of the grid used to generate the turbulent flow field. (Please see **Section §3** for details of the experiment including specifics of the turbulence grid and how correlation was measured and calculated.) The measurements of Stewart and Townsend are also shown for comparison. Their results consists of three different turbulence grids. Although their data has significant scatter, it can nonetheless be said to provide a markedly different transverse correlation than that measured in this current experiment.

Of particular interest for the study of turbulence is how the transverse correlation behaves towards very large separation, and in particular how the negative correlation recovers and asymptotes towards a constant value. Therefore, Figure 2 provides a closer view of this

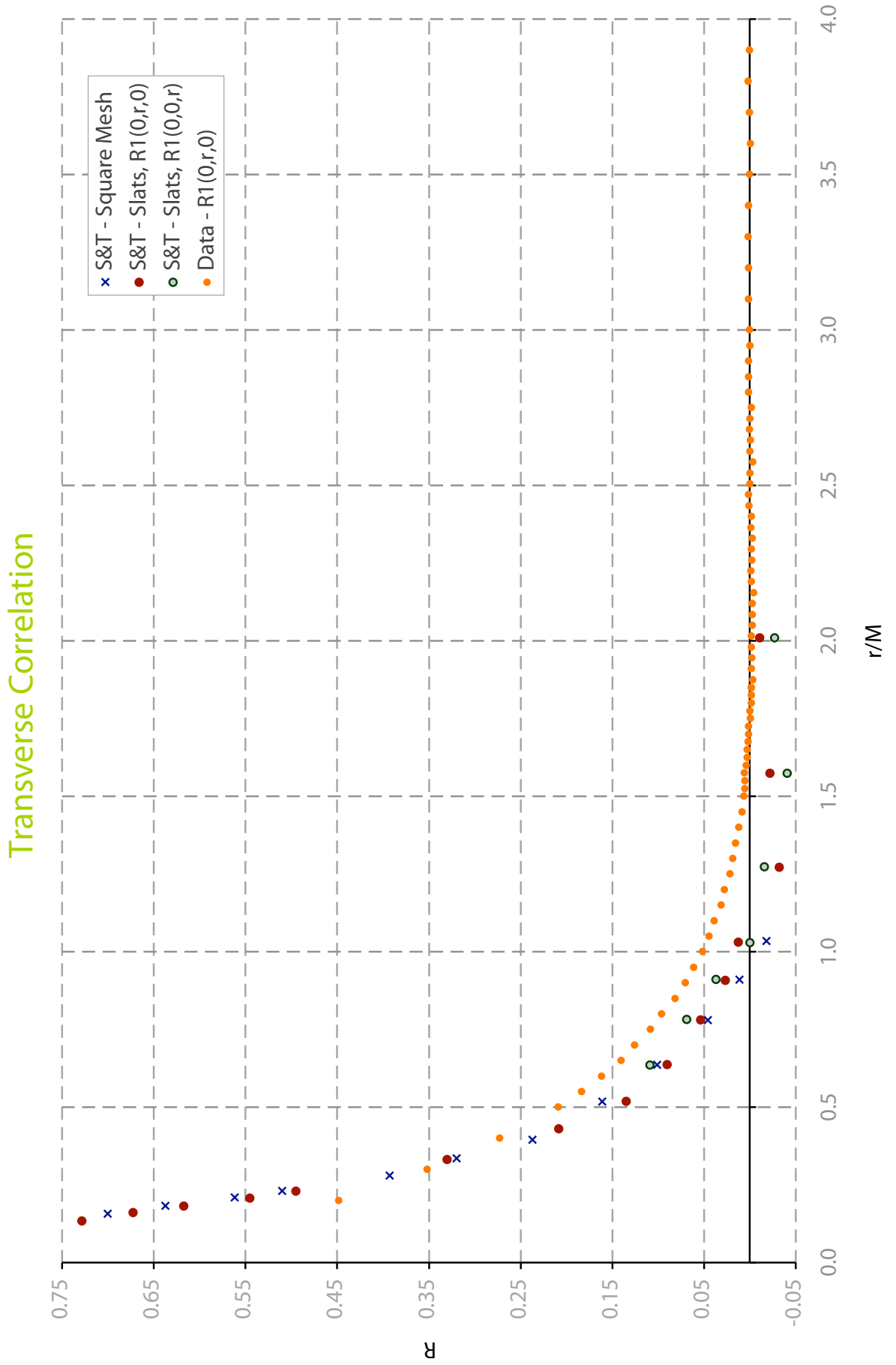


**Figure 1:** The measured transverse correlation data compared to the results of Stewart and Townsend [1]

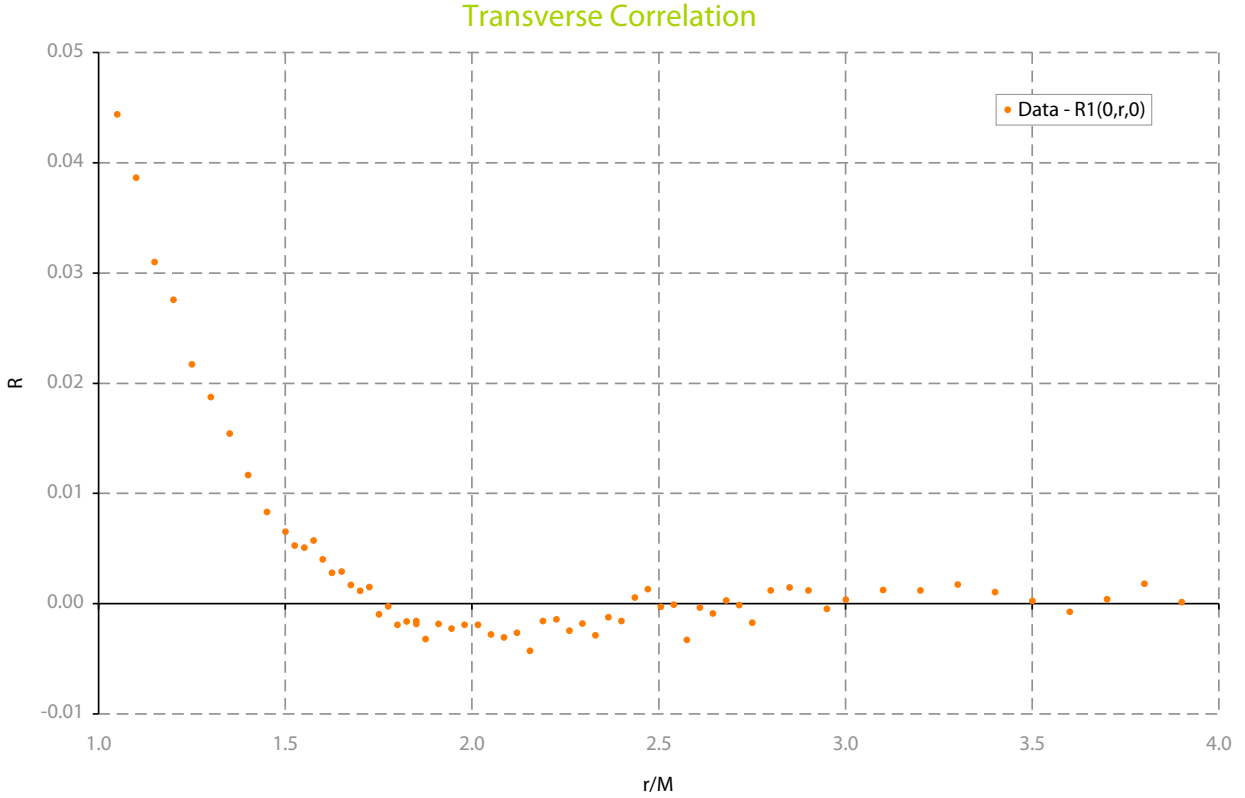


**Figure 2:** Detail of the measured transverse correlation data

behaviour. The unreliability of the data due to the low signal-to-noise of the measurements becomes evident at this scale. Nonetheless, the measurements exhibit some reassuring traits supporting the notion that the transverse correlation of the turbulent flowfield was at least partially successfully observed. In particular, the correlation is observed to drop to negative - albeit small - values and then gradually recover. Although the scatter is quite large, it is not inconceivable that at values of  $r/M$  greater than  $\sim 2.75$  the correlation is fluctuating about some constant value.

### 3 Experimental Apparatus and Method

The actual experimental apparatus and the method ultimately used to produce these results are described first in the following subsections. The wind tunnel, turbulence grid, probe holders, and traverse system are described in 3.1 Experimental Hardware. The following section, 3.2 The Measurement Chain and Method, focuses on the signal from the hot-wire probes and how it is processed and analysed to ultimately provide the correlation.

While this was the procedure ultimately followed, many alternative methods were tested and their validity evaluated; this information is presented in the embedded subsections and provides a rationale for why the final method was chosen. Various sensitivity studies

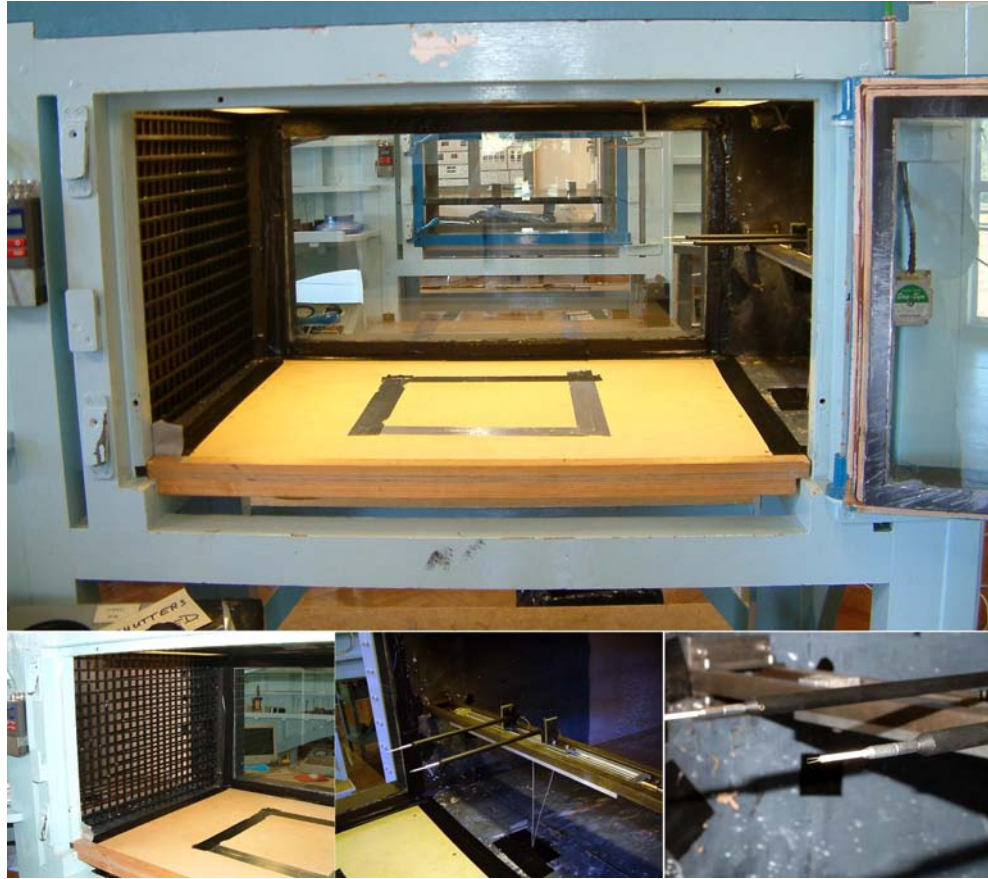


**Figure 3:** A photograph depicting the experimental setup

lend insight into the problems associated with measuring the low signal-to-noise transverse correlation and show the relative importance of different factors.

### 3.1 Experimental Hardware

The experimental setup is depicted in Figure 3. The measurements were made in the University of Cambridge Department of Engineering 1A open circuit wind tunnel. The test section has a cross section of  $71.5\text{mm} \times 52.9\text{mm}$ . The tunnel test section is *not* at atmospheric pressure so care had to be taken to seal any gaps or openings. No tapering of the test section is provided to account for the growing boundary layer so it is possible that there is a slight longitudinal buoyancy due to the decrease in effective cross-sectional area. The empty tunnel freestream turbulence intensity was measured to be 0.125%.

The tunnel was observed to suffer from unsteady speed control. This was probably due to the old, simple speed-control electronics rather than any aerodynamic effect, though open-circuit “suckdown” tunnels in confined spaces are known to occasionally suffer from odd aerodynamic behaviour including pneumatic-compression oscillations (if the venting volume is too small) or possibly inlet vortex formation from the ground.

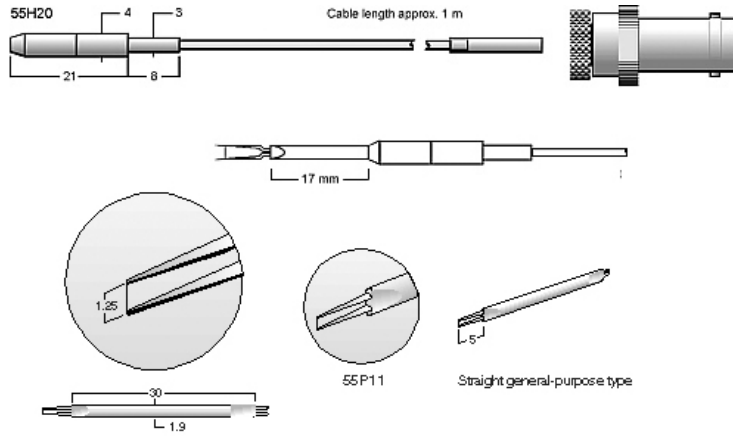


**Figure 4:** Details of the Dantec 55P11 hot-wire probe and Dantec 55H20 probe holder.

A grid was installed at the end of the contraction/inlet to the test section to generate a turbulent flowfield and can be seen in the lower-left inset of Figure 3. The grid was made of  $0.25'' \times 0.25''$  brass square rods tack-welded together to form a  $1.25''$  on-centre square grid. This results in a 64% open area. At maximum power, the tunnel was able to operate at a freestream velocity of  $14.5\text{m/s}$  with this blockage.

When required, a pitot-static tube was inserted into the freestream. The pressure from this probe was measured using a PTX-650 pressure transducer and sampled by the data system. The pitot-static tube is just visible in the top of the ceiling of the test section in Figure 3. When not required the probe was retracted so as not to disturb the flow.

The transverse correlation was measuring using two identical Dantec 55P11 Constant Temperature Anemometry (CTA) hot-wire probes mounted in Dantec 55H20 straight probe holders. The details of the probe and holder are presented in Figure 4. (The details of the entire measurement chain are provided after the hardware and traverse system.)

The two hot-wire probes were installed in custom made probe holders, visible in the central and right insets in Figure 3. The holders were made of  $3/8''$  brass tube and chosen so as to be rigid and not contribute to vibrational-motion noise in the signal. The tips of the hot-wire probes are over  $200\text{mm}$  from the traverse and this was chosen so as to avoid any upstream aerodynamic influence from the base or traverse. These probe holders were mounted to the trolleys on the traverse using rigid steel angle-brackets. This arrangement was chosen so as to permit the smallest separation possible. The probes were located approximately  $74\text{cm}$  downstream of the grid.

The traverse itself was a Velmex A1518C-S1.5-LR-RC dual drive nut traverse visible in Figure 3. Details of the traverse are provided in Figure 5. The two drive nuts are installed with opposite thread directions so that rotation of the lead screw results in precise contrary motion of the trolleys. The trolleys are guided in precise tracks and there is minimal back-

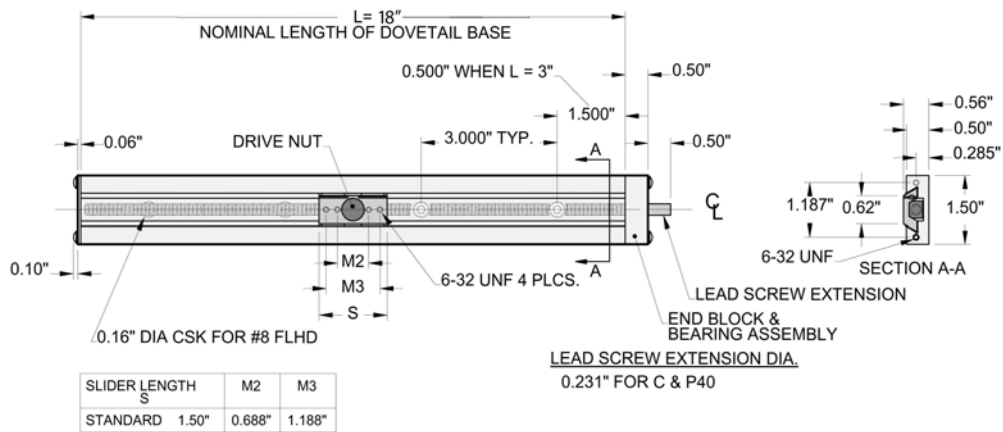


**Figure 5:** Details of the Velmex dual-trolley contrary motion lead-screw traverse

lash. The traverse was mounted in the tunnel using  $5/8''$  square steel rods, again chosen to minimise any vibration or motion of the traverse.

The pitch of the lead screw is  $0.05''/rev$ . A counter is installed on the end of the traverse which provides  $1/10th$  of a revolution precision. In order to automate the data-gathering process, the traverse was automated. This was achieved by installing a Sanyo-Denki size 23 stepper motor on the end of the lead screw. This was in turn controlled by a GSM4 Intelligent Stepper Controller system. Using half-steps, the relative precision of the motion system was 400 steps per revolution, or 1.25 thousandth of an inch, although ultimately the absolute accuracy of the traverse was limited by the measurement of the offset between the two probe tips and in the second order by the accurate reading of the traverse counter.

The stepper system did not provide feedback of motor position, so the traverse counter needed to be used with a man-in-the-loop method to initialise traverse position. In order to make the traverse counter visible outside the tunnel a webcam (visible in the centre of Figure 6) was mounted inside the test section. An image of the counter was presented to the operator on a computer screen.

The entire measurement process was automated. The test management program was provided with a map consisting of the various  $r/M$  points at which a correlation was desired. The program would move the traverse to this point, the measurements made according to the predetermined method (see following section) and when complete, the traverse went on to the next point.

### 3.2 The Measurement Chain and Method

It was known from the outset that one of the greatest challenges in measuring the transverse correlation was the low signal-to-noise ratio. Consequently, significant effort was expended



**Figure 6:** Photographs of the instrumentation and webcam monitoring of the traverse position

in minimising noise and preserving the signal.

The measurement chain is depicted in Figure 7. The individual components of the measurement chain are described below, as is the data analysis used to calculate the correlation.

**Hot-Wire Probes/CTA System:** The Dantec 56C01 CTA System with CTA Bridge 56C017 was carefully optimised to provide the best possible signal from the 55P11 hot-wire probes. The bridge circuit underwent both static and dynamic bridge balancing. The overheat ratio,  $a$ , was 0.9 and the dynamic response of the hot-wire system was confirmed up to around 55kHz.

**Kemo High-Pass Filter:** The signal from the CTA was passed through a two-channel Kemo filter box; the filters were operated in discrete mode and each hot-wire signal was handled separately. The High-Pass filter was set to 5Hz, with a 36dB/Octave attenuation. The resulting signal was thus AC coupled, though due to the nature of the filter box there was a slight DC offset on the order of 30mV on Channel 1 and 47mV on Channel 2.

**Fylde FE-351-UA Data Amplifier:** The Fylde data amplifier is a very-low noise, high-accuracy, stability and linearity, high CMR and wide-dynamic range device; it performed three functions. First, the unit had an optional 30kHz, fourth-order Butterworth low-pass filter installed. This served to remove high-frequency noise in hot-wire signal, and was chosen to be below the maximum response of the hot-wires themselves. Next, the amplifier provided a gain of 50 to the signal. This was carefully chosen based upon a typical signal from the probes and selected so that it filled the 16 bit window of the data system when the input range was selected to be  $\pm 2.5V$ . Finally, the amplifier also provided a DC offset that was used to account for the slight offset due to the Kemo filter box.

**ComputerBoards PCI-DAS16/20 Data Acquisition Board:** The signal from both hot wires then went to a custom built breakout box that routes signal into a PCI card in

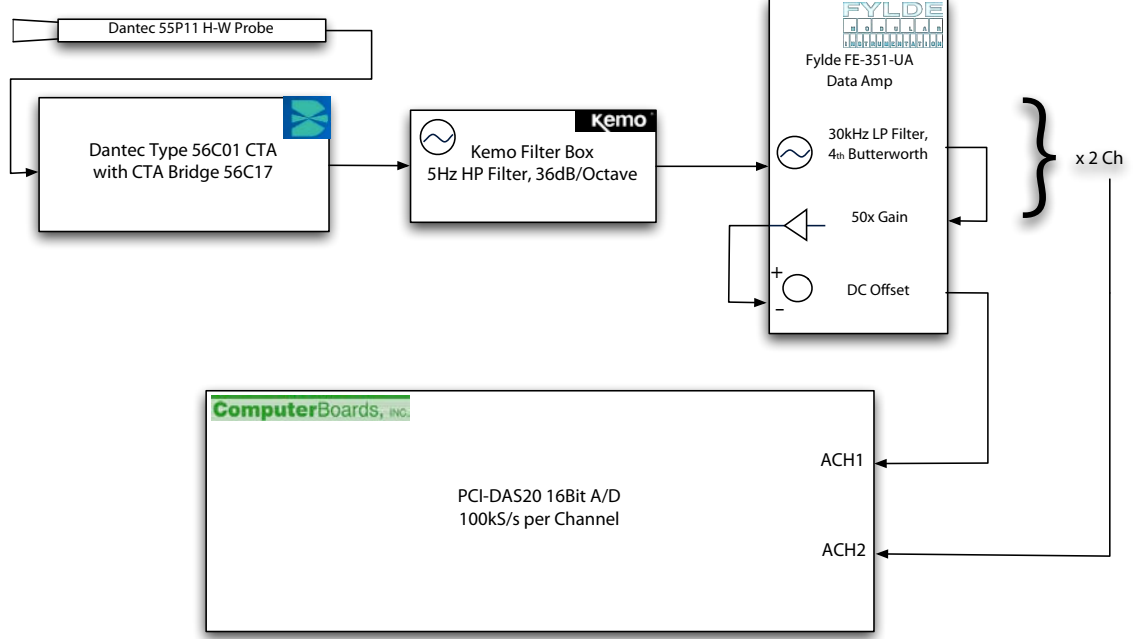


**Figure 7:** A schematic illustrating the measurement chain

the computer. This data acquisition card provided 16 bit resolution and differential input for each channel. The hot wire signals were each sampled at 100 000 samples per second. This was more than the Nyquist sampling frequency required by the signal. Instead, the driving motivation was to minimise the effect of non-simultaneous sampling (see Section 3.3, Non-simultaneous Sampling). At 100kS/s, the phase delay between the sampling of the two signals was limited to  $20\mu\text{s}$ .

**Calculating the Transverse Correlation:** The transverse correlation (in terms of  $r/M$ ) of streamwise velocity, is given by:

$$R_1^1(0, \frac{r}{M}, 0) = \frac{\overline{U_1' \cdot U_2'}}{\sqrt{\overline{U_1'^2}} \cdot \sqrt{\overline{U_2'^2}}}$$

If the range of the velocity is small enough, then the hot-wire probes can be assumed to respond linearly to the velocity fluctuations. In this case, the velocity fluctuation can be rewritten simply as:

$$U_1' = k_1 E_{01}'$$

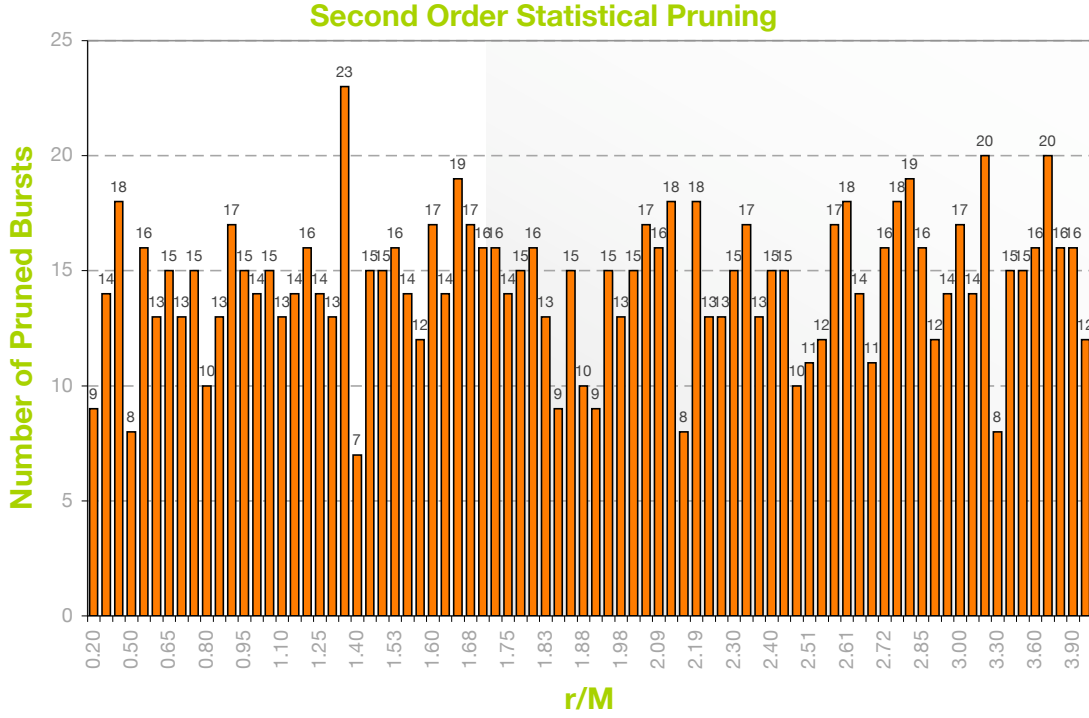


**Figure 8:** The number of casualties suffered at different  $r/M$  due to the second-order statistical pruning.

Then the correlation can be expressed simply in terms of the voltage fluctuations of the CTA system:

$$R_1^1(0, \frac{r}{M}, 0) = \frac{\overline{E'_{01} \cdot E'_{02}}}{\sqrt{\overline{E'^2_{01}} \cdot \overline{E'^2_{02}}}}$$

Theoretically for an AC coupled signal, the voltage coming from the CTA should be the fluctuation voltage itself. However, due to the slight offset in the signal throughout the measurement chain, the mean value needed to be calculated first and then subtracted from each data point to get the true fluctuation voltage.

**Measurement and Data Analysis:** At each  $r/M$  the correlation was determined by measuring a total of 300 bursts, each burst being 5 seconds in duration. As described in the previous paragraph, the fluctuation voltage,  $E'_0$ , was calculated using the mean voltage within that particular burst. For each burst, three components of the correlation were calculated and recorded to a log file; the raw data was discarded. These components were:

$$\overline{E'_{01} \cdot E'_{02}}$$

$$\overline{E'^2_{01}}$$

$$\overline{E'^2_{02}}$$

In order to piece all the bursts together and calculate correlation, the different values for each component were averaged together, and then these mean values used to calculate the overall correlation.

However, this was not sufficient; a further step was taken to prune the data set before calculating the final correlation. When looking at the statistics of the bursts, it was noticed that there was a significant scatter of some of the data points. Therefore it was decided to eliminate bursts that fell outside of  $\bar{x} \pm 2\sigma$ . Here, the mean,  $\bar{x}$ , and standard deviation,  $\sigma$ , are calculated using the “instantaneous correlation” for each burst; that is to say the correlation calculated using that burst alone.

It was also noticed that very occasionally a burst would produce impossibly large correlations. In these cases, applying only a single pass of the pruning algorithm would only remove this one, extremely deviant point while sparing points that otherwise would be considered unsuitable. Therefore, a second pass of the pruning was applied. Thus, the post-processing of the data set was termed “second-order statistical pruning”.

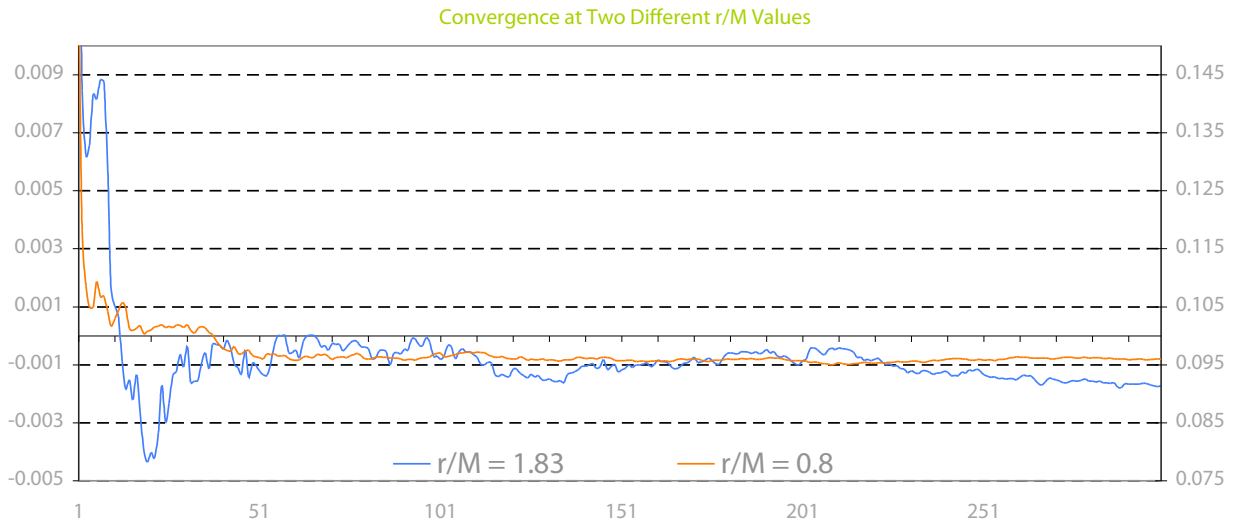


**Figure 9:** Convergence of the data

The convergence of two data points are shown as an example in Figure 9. The x-axis represents the 300 bursts measured to determine the correlation. The correlation as calculated up to the given burst is plotted. For the data set at  $r/M = 0.8$ , the data converges rather quickly. At the larger separation of  $r/M = 1.83$ , the convergence is less convincing. In fact, there is a question of whether the final value is indeed converged. No exhaustive study of convergence was made; these two points were selected at random.

### 3.3 Method Optimisation: Sensitivity Studies

There are a large number of potential variables that can influence the measurement chain and very little literature or knowledge on how they might be expected to affect the final results. Therefore, a program of sensitivity studies was undertaken to explore each variable. Each was studied in isolation, adjusting only one variable at a time thus isolating its effect.

**Baseline:** To begin with, a baseline study was conducted (different than the final method used for the master data) in order to provide a standard against which all subsequent variations could be benchmarked. This consisted of taking 200 bursts of 5 seconds each over a range of  $r/M$  values between 0.2 and 2.4 in increments of 0.1. There was no High-Pass filtering used. The amplifier was adjusted to maximise the sampling window; the 30kHz low-pass filters in the Fylde amps were active. The hot-wire probes were calibrated and the correlation done using the scaled velocities. There was a first-order statistical pruning of data outside of  $\pm 2\sigma$ .

**Sensitivity to Leaks in Tunnel:** A concern with non-atmospheric test-section wind tunnels is that if the walls are not airtight then the low-pressure inside will draw air in. This incoming jet can influence the measurements in the test section and possibly even interact with the boundary-layer growing on the tunnel walls which could in turn lead to even greater disturbances. The baseline run was repeated with as many of the openings and gaps around the test section sealed as possible. There was no visible difference in the correlation or the quality of the measurements. Nonetheless, this sealed configuration was adopted for the final measurement.

**Number of Bursts and Burst Length:** The signal to noise ratio of the correlation was very poor, especially at large  $r/M$ , so a long sample time was needed. However, the computer was unable to store the 2 channels of 100kS/s 16 bit data for more than half a minute or so. Therefore it was decided to instead measure several bursts of shorter duration and posthumously consolidate the individual bursts for the final measure of correlation.

If the signal is not AC coupled then the burst size effectively acts as a High Pass filter. This is because the fluctuation velocity within a burst is calculated using the mean flow of that burst alone. A longer burst might experience significant mean-flow fluctuations due to, for example tunnel unsteadiness, that will skew the mean value. A shorter burst is less likely to see this effect.

In order to gauge the effect of different burst lengths and numbers of bursts, several points of the baseline graph were repeated. First, 200 samples were made using 1 second bursts, for a total sampling time of 200 second per data point, compared to 1000 seconds per point in the baseline. The second case was made using 10 second bursts and 200 samples

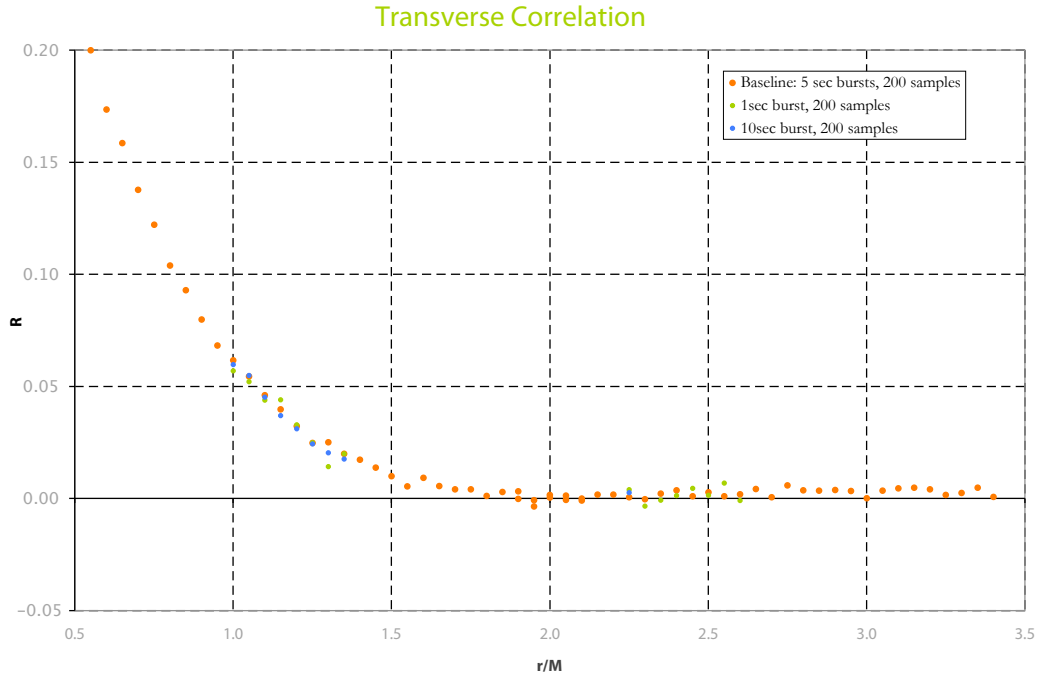


**Figure 10:** Sensitivity Study: effect of burst size on correlation

for a total sampling time of 2000 seconds.

The results are shown in Figure 10. There is no wholesale, dramatic difference between any of the three cases. The most notable difference is in the relatively poor quality of the 1 second burst size. This is probably due to the fact that there is a large difference in the seconds of data for the different cases. Indeed, the 1 second burst case is seen to have several points with very poor convergence. Yet ultimately, it was concluded that burst size did not have a significant effect on the correlation. This becomes even more the case when the signal is AC coupled. In this case, the burst size can be driven by data acquisition and computing demands.

**$E_0$  Versus V Correlation:** The original baseline run calculated the correlation based on scaled velocity. This involves calibrating the probe and converting the raw voltage into velocity. Using the voltage for calculating the correlation is not only simpler, but it would allow for using a high-pass filter (i.e. AC coupling the signal) and a more flexible - and consequently more effective - approach to optimising the sampling window.

As discussed in Section 3.2, if the velocity fluctuations are small enough that the sensitivity of the probe measured in volts is effectively linear, then it is valid to calculate the correlation using  $E_0$  rather than velocity. To verify this assumption, the correlation at three different separations was measured using 200, 5 second bursts at each point. The correlation was simultaneously calculated for each burst based on both calibrated velocity and raw voltage. This is shown in Figure 11, and as can be seen, there is no large-scale significant

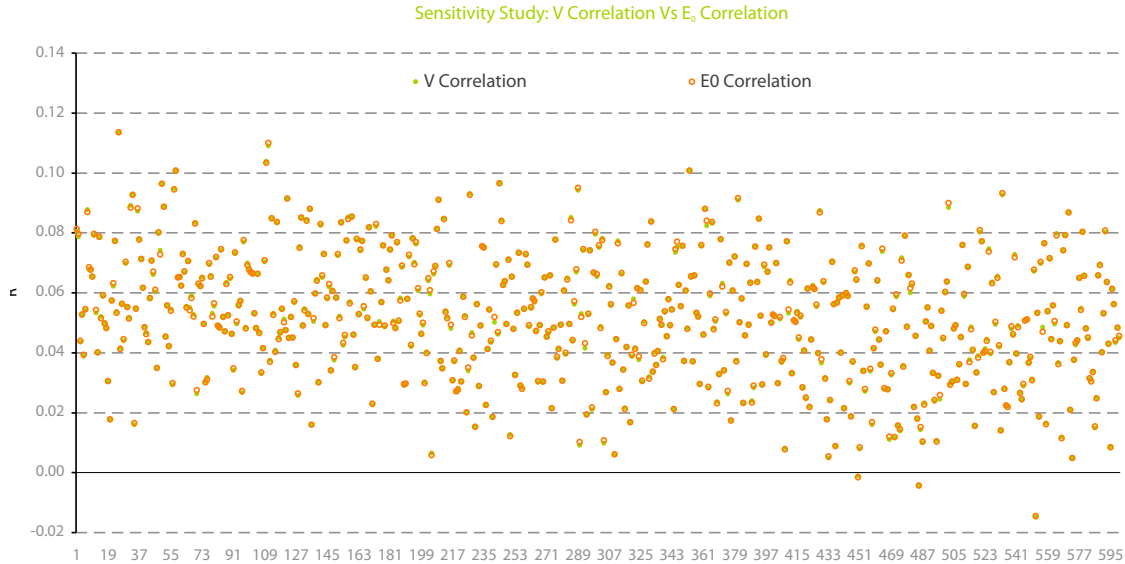


**Figure 11:** Effect on correlation of using the raw voltage,  $E_0$ , or the calibrated velocity,  $V$ .

error associated with basing the correlation on the raw voltages. The very small discrepancy that does exist is probably due to the slightly stale calibration used for the scaled velocities. It was concluded that the advantages of using  $E_0$  correlation far outweigh any problems.

**High-Pass Filtering:** Once it was determined that it is feasible to base the correlation on raw voltages, it became possible to consider using high-pass (HP) filtering on the hot-wire signal. This would have the effect of AC coupling the signal, thus removing the need for large DC offset. The gain on the amplifiers can then be adjusted precisely to fill the sampling window. Also, the use of HP filtering would remove any background correlation due to low-frequency oscillations in the tunnel; any large unsteadiness of the tunnel would be correlated and possibly drown-out the true signal.

In order to quantify the effect high-pass filtering would have on the correlation, several points of the baseline run - some around  $r/M = 1.25$  and other around  $r/M = 2.4$  - were measured using different high-pass filter settings. The three settings tested were  $0.1Hz$ ,  $1.0Hz$ , and  $10Hz$  with  $36dB/Octave$  attenuation. The results are shown in Figure 12.

As can be seen, the effect is quite pronounced. In particular, having a fairly high HP filter setting at  $10Hz$  makes a large difference compared to even the  $1Hz$  filter. This would seem to suggest that a large part of the correlation of the signal is coming from between 1 and 10 Hz. It is questionable whether this correlation is a legitimate feature of the turbulence correlation or simply some artefact of the experimental apparatus. To put things into perspective, the data of Stewart and Townsend is also shown in Figure 12. And while the effect of the  $10Hz$  filter is large, it is not on the order of the difference between the results.

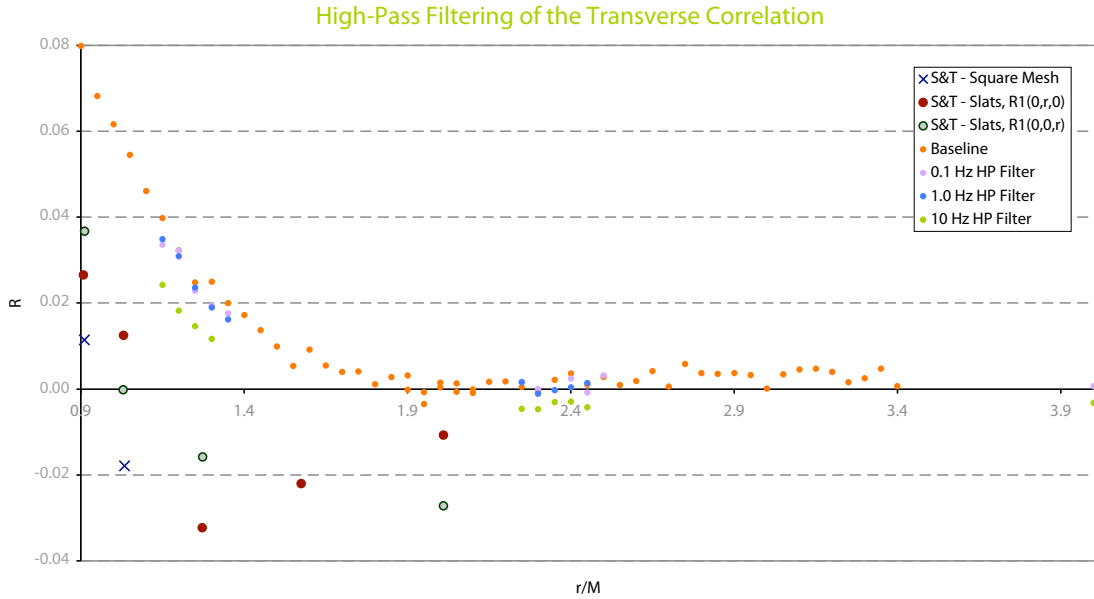


**Figure 12:** Effect of high-pass filtering the hot-wire signal. Stewart and Townsend [1] data is included for comparison.

This issue needs to be explored in more detail. For example, what is the lowest frequency of the flow that can be considered to be a legitimate component of the turbulent flow? What happens if the HP filter is set to an even higher value? Is the effect of the HP filter at, say 10Hz, simply a constant mean offset in the correlation or does it vary with separation? Does the use of an HP filter improve the quality of the measured data, in particular its standard deviation and convergence?

**Non-simultaneous Sampling:** The PCI-DAS20 is capable of measuring a maximum of 200000 16 bit samples per second (S/s) on a single channel. However, the board is not capable of simultaneous sampling and thus if two channels are to be sampled at the same time, then not only is the sampling rate reduced to 100kS/s, but there is a 50kHz phase shift between the two channels. This corresponds to a  $20\mu\text{s}$  delay in measurements between the two channels.

While this has little effect on the validity of the measured signal on a per-channel basis, if the objective is to conduct phase-sensitive calculations between the two signals, such as, for example, a correlation, then there is a significant effect; the final correlation will be artificially influenced as a function of the frequency of the signal. In the current case, for example, a correlated signal of 50kHz present on both channels would appear to be  $90^\circ$  out of phase and thus would appear to have a correlation of 0. A signal of 100kHz would be  $180^\circ$  out of phase and would actually register a correlation of  $-1$ .

In order to verify this experimentally, a signal generator was used to generate a signal consisting of a single sine wave at a known frequency. This signal was fed into both channels

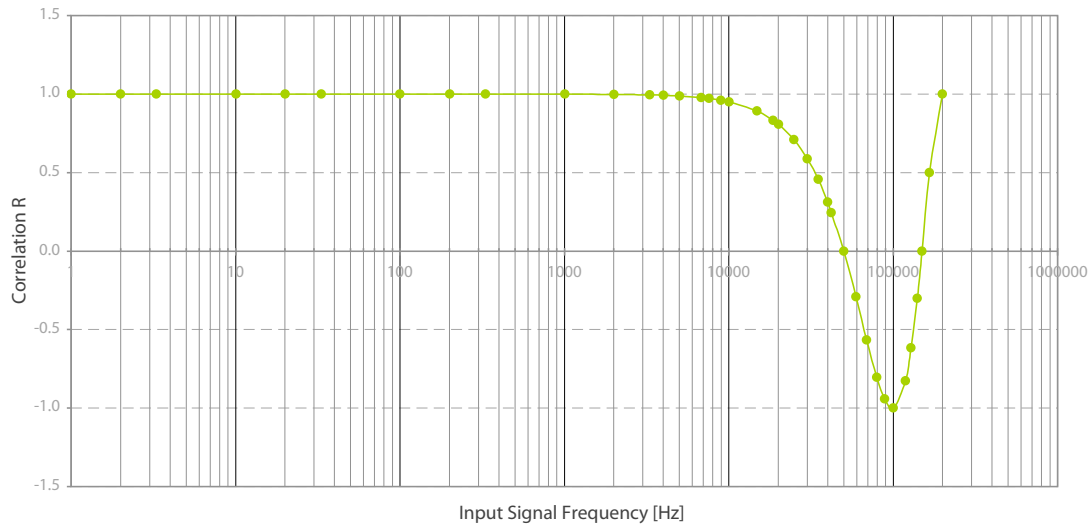


**Figure 13:** Effect on correlation as a function of frequency of signal due to non-simultaneous sampling. Each channel sampled at 100kS/s, with a  $20\mu\text{s}$  delay between channels.

of the data system and correlated. The result is shown in Figure 13. Ideally, this should yield a correlation of 1 irrespective of the frequency of the signal. As expected, at low frequencies the signal appears perfectly correlated. However, as the frequency increases to around 10kHz, there correlation is slightly attenuated. By 30kHz the correlation of the signal appears to be only approximately 0.5 due to the  $20\mu\text{s}$  delay between channels of the non-simultaneous sampling.

The effect of this behaviour can be quite significant. High-frequency signals will be under-correlated or actually show a negative correlation. In the current experimental setup, the 30kHz low-pass filter in the amplifier stage should mean that there is very little information at higher frequencies. Nonetheless, if the turbulent flow has significant information between the range of 10kHz-30kHz then it will be under-correlated. One solution would be to use a data acquisition board capable of simultaneous sampling. Alternatively, a board with a very high sampling rate will be able to accurately measure correlation to much higher frequencies without attenuation. For example, a 1.5MS/s board would only have a  $2.67\mu\text{s}$  delay between channels. Presumably, such a system would be able to correlate a signal up to 75kHz with minimal attenuation.

**EM Noise:** Hot-wire probes are known to be very sensitive to electromagnetic (EM) noise. The experiment was subjected to several sources of EM noise: the main fan drive system, the fluorescent lighting tubes in the test section, the CRT monitors used by the data system, and the stepper motor and control system. For obvious reasons, disconnecting the main fan drive system was not an option. However, the other systems could be disabled whilst

---

measurements were made. For example, the two CRT monitors were observed to induce a strong signal at  $56.45\text{kHz}$  and  $60\text{kHz}$ ; this noise was induced in the measurement train *downstream* of the various filters! Likewise, stepper systems used elsewhere in the laboratory radiated unacceptable levels of noise. For this reason, the current GSM4 stepper system was specifically selected for low-EM operation and did not induce any observable noise in the hot-wire system.

In order to ascertain whether these sources of EM noise had any significant effect on the final transverse correlation measurements, various points of the baseline test were repeated with the mentioned systems turned off. The results suggested no consistent, demonstrable effect of this EM noise on the final correlation. Neither the mean values nor the standard deviation of the values was altered in a consistent manner. This is probably due to the natural attenuation of the non-simultaneous sampling at the high frequencies in question (see above).

## 4 Conclusion

This technical report documents in detail the steps that were taken to measure the transverse correlation in a homogenous turbulent flow. However, the final results currently are not the definitive word on the subject that it was hoped it would be. In particular, the quality of the data at large separations is poor and shows what appears to be some systematic oscillation. Also, the marked difference between the current data and Stewart and Townsend has not been adequately explained.

In particular, the following points still need to be addressed:

1. **Waviness at large Separation:** It was suggested that the waviness of the transverse correlation at larger  $r/M$  seen in Figure 1 might represent artefacts of the turbulence grid, despite “conventional experimental wisdom” suggesting that at the downstream distance used in the experiment there should be no influence felt from the grid. This theory gains credence when looking at the “*Baseline*” measurement made for the sensitivity studies, shown for example in Figure 12. Although measured at a different time using different methods, this graph also shows the same waviness. This would suggest that a different grid in a different tunnel would present a different correlation. More work needs to be done in understanding the effects of different screens.
2. **Frequency Spectrum of Phenomena:** The experience with using the high-pass filters suggests that the frequency spectrum of the problem is not well understood. This specifically refers to both the spectra of the turbulence and of the correlation. As discussed in the text, it appears that a significant portion of the correlation occurs at very low frequencies. Likewise, the effects of non-simultaneous sampling would suggest

that any significant high-frequency signal would be under-correlated. This nuance needs to be understood before the overall topic can be put to rest.

Fortunately, this is something that can be studied right now. Over 150 seconds of the full time-dependant raw signal measured at two different separations are available from the author.

3. **Systematic Background Correlation:** Any systematic background correlation would have the effect of providing a constant mean offset in the correlation plot. However, if this background was even slightly a function of separation then it would in all likelihood drown out the fine details of the transverse correlation at large separations. This specifically ties into the two previous comments and raises the question of whether the imperfect grid or the frequency spectra are a function of separation.
4. **Miscellaneous Aerodynamic Effects:** Insufficient effort was put into quantifying and nailing down the influence of aerodynamic features. This includes things like the aerodynamic influence of the probe holders, the traverse, the unsteady tunnel and even features of the tunnel such as the longitudinal pressure gradient due boundary layer growth.

Taking a step back and casting a objective eye over the accomplishments of the project at the strategic level, one can argue that while significant effort has been invested in pursuing the question of how to measure the correlation, insufficient effort has been expended at verifying the aerodynamics of the problem. In other words (with the possible exception of the effect of HP filtering and frequency spectra) the author has very high confidence that the results presented in Figure 1 is a very close measure of the transverse correlation in the experiment. However - and this is key - it is far from certain whether the correlation measured is really that of an isotropic, homogenous turbulent flow.

If this work is to be continued, it is suggested that first, before any more time is spent making measurements, the frequency information referenced in the Appendix is examined and at least a rough effort made at understanding the spectrum of the correlation. Secondly, the effect of different turbulence generating screens needs to be quantified. Finally, some work should be done on looking at both minor aerodynamic effects (such as probe holders and traverse) and major aerodynamic effects (such as tunnel influence, even if this means repeating the measurements in a different tunnel).

## References

- [1] STEWART, R.W., & TOWNSEND, A.A. 1951 "Similarity and self-preservation in isotropic turbulence", *Phil. Trans. Roy. Soc. A* **243**, 359

- [2] DAVIDSON, P.A. 2004 “Turbulence: An Introduction for Scientists and Engineers”, *Oxford University Press*

## A Appendix - Raw Data

The data files are available for download from the author. The various files are described here.

The raw data measured during the final master correlation is stored in:

`\Appendix\Raw Data`

The measurements were made in two parts; the first run went from a normalised separation of 0.201 up to 1.851, and the second run went from 1.851 to 4.000. (The one point at 1.851 was overlapped to verify repeatability.)

The files labelled `Master01.txt` and `Master02.txt` provide the raw, unprocessed correlation at each separation in a tab-delimited text file, based on all 300 bursts regardless of their suitability. This was used mostly to serve as a quick check whereas the “LOG” files were used to store all the data.

The files labelled `Master01LOG.txt` and `Master02LOG.txt` are also tab-delimited text files. This file contains all the information needed for the data reduction. The first row is the header containing the date and time when the run was started. The remaining rows correspond to all of the individual bursts measured during the run, hence there are over 10000 rows of data in each “LOG” file. These are grouped in sets of 300, corresponding to the 300 bursts measured at each separation.

The first column is the separation in inches. The second, third and fourth column correspond to the three components of the correlation discussed in Section 3.2:

$$\overline{E'_{01} \cdot E'_{02}}$$
$$\overline{E'^2_{01}}$$
$$\overline{E'^2_{02}}$$

## B Final Data

The processed, final data is also available from the author. They are found in the directory:

`\Appendix\Final Data`

The raw data underwent the second-order statistical pruning described in Section 3.2. The Matlab program to do this is included as `PruneData.m`. The two “LOG” files were

processed and the colated results can be found in the tab-delimited text file `FinalData.txt`. In this file, the first column is the normalised separation,  $r/M$ , the second column is the correlation for that separation calculated using only the valid bursts, and the final column is the number of bursts that were considered deviant and were thus discarded.

## C Stewart and Townsend Data

The original data from Stewart and Townsend was extracted by scanning their plots and digitally calculating the data points. The numbers and a plot of their reconstructed data is included as a Microsoft Excel spreadsheet file:

```
\Appendix\Final Data\Stewart and Townsend.pct_da.xls
```

## D Time History

In general it was not possible to save the actual raw sampled data since at each burst this consisted of 1000000 16-bit integers *per each burst* times three hundred bursts times 84 separation points. However, some time history data was kept and is included in the Appendix so that it can be analysed at a later data for such information as spectrum of the turbulence and the spectrum of the correlation.

This data can be found in:

```
\Appendix\Time History
```

For this data, two different separations were looked at. At each separation, 15 bursts were recorded in their entirety. Each burst was 10 seconds long, sampled at 100kS/s/channel, 16 bit raw data, with the 0.1 Hz HP filter used (so as to maintain low-frequency signal components and yet still provide an AC coupled signal). The 30kHz LP filter in the data-amps was still used. The data is stored as a raw text file. In each file, the raw data for each channel is interleaved and alternates from row to row. In otherwords, the first row is the sampled voltage of CH1 then the second is the sampled voltage for CH2 and so on. These files are very large and contain  $2 \times 10^6$  rows corresponding to 10 seconds of 100kHz data for each channel. They are therefor not amenable to being opened by a typical spreadsheet application, for example.

The nomenclature for the files is:

files A01.txt through A15.txt is the raw frequency data for  $r/M=1.25$

files B01.txt through B15.txt is the raw frequency data for  $r/M=2.3$